\$ SUPER

Contents lists available at ScienceDirect

Environmental Pollution

journal homepage: www.elsevier.com/locate/envpol





Estimating the seasonal and spatial variation of urban vegetation's PM_{2.5} removal capacity[†]

Wei Yang ^a, Wenpeng Lin ^{a,b,*}, Yue Li ^a, Yiwen Shi ^a, Yi Xiong ^a

- a School of Environmental and Geographical Sciences, Shanghai Normal University, Shanghai, 200234, China
- ^b Yangtze River Delta Urban Wetland Ecosystem National Field Scientific Observation and Research Station, Shanghai, 201718, China

ARTICLE INFO

Keywords: PM_{2.5} Urban vegetation i-Tree eco Local Climate Zone (LCZ) Spatiotemporal variability

ABSTRACT

Fine particulate matter (PM2.5) is one of the most severe factors contributing to urban air pollution, posing significant risks to human health and environmental quality. Urban vegetation, acting as a natural method for pollution mitigation, can effectively reduce harmful air particle concentrations through processes like adsorption and deposition. While much research has quantified urban vegetation's role in PM25 removal, the spatial variability and seasonal fluctuations of this process in urban environments remain poorly understood. Furthermore, few studies have quantitatively explored the environmental factors that influence this capability. Using Shanghai as a case study, this research estimates the PM_{2.5} reduction by urban vegetation in 2022, integrating the i-Tree Eco model with Local Climate Zones (LCZs) classification. The results indicate that vegetation plays a significant role in PM_{2.5} removal, with a total annual removal of 835 tons and an average removal rate of 0.51 g m^{-2} year⁻¹ per unit leaf area. The maximum annual air quality improvement reached 21.7%, with an average of 4.09%. The removal flux exhibited a clear "double peak" pattern throughout the year, with peaks occurring in late spring and late summer. Significant spatial variations in PM2.5 removal capacity were observed across different LCZs, ranked as follows: Dense Trees > Open Lowrise > Large Lowrise > Bush/Shrub > Scattered Trees > Others. Notably, Open Lowrise areas demonstrated considerable potential in both removal flux and total removal. The 38-42 mm evapotranspiration range was found to be the most effective for PM2.5 removal. However, when evapotranspiration exceeded 50 mm, removal efficiency showed a clear diminishing marginal effect, closely linked to the regulation of leaf stomatal opening and closing. The findings of this study underscore the importance of vegetation in improving air quality and provide valuable insights for urban planning and environmental policy.

1. Introduction

The rapid pace of urbanization globally has brought numerous challenges, with the deterioration of air quality being especially prominent. Fine particulate matter (PM $_{2.5}$), measuring 2.5 µm or less, can penetrate deep into the human lungs (Feng et al., 2016; Yang et al., 2020) and even enter the bloodstream, posing serious risks to public health (Yin et al., 2018; Seposo et al., 2018). In recent decades, this issue has garnered significant global attention (Wang et al., 2020; Huang, 2023). In response to this challenge, numerous studies have explored methods to address PM $_{2.5}$ pollution from various perspectives, with most focusing on source control (Zheng et al., 2019). However, given the limitations of controlling pollution sources, it is crucial to find new

pollution reduction strategies. In this context, urban vegetation, as a natural air purification tool, has attracted significant attention from researchers for its ability to reduce $PM_{2.5}$ (Wu et al., 2019). Urban greenery not only beautifies the environment but also removes airborne particles through multiple mechanisms, including dry deposition on tree leaves and branches (Zhang et al., 2020; Su et al., 2020), stomatal uptake (Choi et al., 2021), and chemical reactions on leaf surfaces (Altimir et al., 2004). Among these, dry deposition is the dominant process, contributing 70%–90% of $PM_{2.5}$ removal by leveraging large vegetation surface areas and aerodynamic processes (Liu et al., 2016; Du et al., 2019). In contrast, leaf absorption makes a relatively minor contribution to $PM_{2.5}$ removal, as it primarily plays a role in the uptake of gaseous pollutants rather than particulate matter.

 $^{^{\,\}star}\,$ This paper has been recommended for acceptance by Dr Alessandra De Marco.

^{*} Corresponding author. School of Environmental and Geographical Sciences, Shanghai Normal University, Shanghai, 200234, China E-mail address: linwenpeng@shnu.edu.cn (W. Lin).

Using models (Jeanjean et al., 2016) to simulate dust retention in green spaces and evaluate their effects is a common research method in environmental science. Among these, the i-Tree Eco model is widely used for dry deposition. Developed by the USDA Forest Service and its partners, this model helps users evaluate and manage tree resources by estimating the contributions of trees and forests to urban and suburban environments (Ristorini et al., 2023; Su et al., 2022). Its dry deposition component (UFORE-D) can simulate the removal of atmospheric pollutants by trees and shrubs during non-precipitation periods, Trang et al. (2022) used this model to evaluate the effect of campus trees on PM particles at several universities in Ho Chi Minh City. The results showed that trees in the campuses of International University and University of Science removed approximately 10 kg and 14 kg of PM2.5 annually, respectively. At the city or larger scale, studies have classified urban tree species and assigned different deposition velocities to different species (Wu et al., 2019), or examined the PM2.5 reduction capabilities of various urban surfaces. Li et al. (2023a) estimated the PM_{2.5} removal capacity of nature-based green infrastructure and explored the impact of different landscape patterns on the removal capacity. Some studies (Corada et al., 2020; Abhijith & Kumar 2020) have also estimated the economic benefits of particulate matter reduction, further demonstrating the significant value of the i-Tree Eco model in urban forest management and policy-making.

These numerous studies (Jeong et al., 2023; Zhou et al., 2019) have primarily focused on estimating the effectiveness of PM2.5 removal and exploring the influence of different vegetation types and configurations (Wu et al., 2019). However, most of these studies are limited to specific points in time and lack systematic analysis of the seasonal variation in urban vegetation's PM_{2.5} removal capacity. In reality, the dust retention capacity of vegetation varies significantly across seasons due to changes in climate and vegetation growth. Ignoring these temporal dynamics fails to provide a comprehensive understanding of the ability of urban vegetation to mitigate particulate matter. While some studies have examined changes in PM2.5 removal by vegetation over multiple years (Li et al., 2023a), they typically focus on long-term trends and do not reveal the specific impact of seasonal characteristics on vegetation's pollution mitigation efficiency. In terms of spatial analysis, traditional land surface classification methods are typically based on land use and land cover (LUCC), for instance, categorizing urban areas into "residential," "commercial," or "industrial" zones. Although this method provides basic physical characteristics, it does not fully capture the complex microclimatic variations within urban areas, especially when evaluating the role of vegetation in PM_{2.5} removal. In contrast, Local Climate Zones (LCZ) classification not only considers surface characteristics but also factors like building height and heat capacity, which influence microclimates. This makes LCZ more effective in reflecting the climatic heterogeneity across different urban areas. In this study, we utilize the LCZ classification to more accurately analyze the PM2.5 removal performance of vegetation in various spatial environments. Although environmental variables such as humidity (Ryu et al., 2019), temperature (Jung et al., 2018), and precipitation have been acknowledged for their impact on removal capacity (Zhang et al., 2017; Yang et al., 2015), quantitative studies on how these factors affect removal efficiency remain scarce.

Therefore, this study uses Shanghai as a case study, applying i-Tree Eco model to estimate the reduction of PM_{2.5} by urban vegetation and analyze the spatial distribution and temporal variation of this reduction capacity throughout 2022. The objectives of this study are: 1) to provide a more accurate estimate of particulate matter removal using the dry deposition model, 2) to determine the spatial distribution and seasonal characteristics of vegetation's removal capacity across different underlying surfaces in Shanghai in 2022, and 3) to explore the impact of surface evapotranspiration on vegetation's PM2.5 reduction capacity.

2. Materials and methods

2.1. Study area

Shanghai is located on the southeastern edge of the Yangtze River Delta (30°40'~31°53'N, 120°51'~122°12'E), where the Yangtze and Oiantang Rivers meet and flow into the East China Sea (Fig. 1). Except for a few eroded residual hills in the southwest, the entire area is a flat, low-lying plain, with an average elevation of around 4 m above sea level. Shanghai has a subtropical monsoon climate, with an average temperature of 15 °C and an annual precipitation of 969.8 mm in 2022, spread across 85 rainy days. The city's greenery primarily consists of urban parks, street greenbelts, residential community green spaces, and suburban forests and wetlands, dominated by evergreen broad-leaved forests and mixed evergreen-deciduous forests. Due to its dense population and high vehicle numbers, PM_{2.5} pollution has been a major focus of Shanghai's environmental management efforts. Particularly in autumn and winter, under adverse climatic conditions, PM2.5 concentrations occasionally exceed standard limits, affecting the health of urban residents (He et al., 2022).

2.2. Data sources and processing

To estimate the removal of air pollutants by urban vegetation in Shanghai, we utilized a dry deposition model (Nowak et al., 2018; Nowak et al., 2006). This model integrates environmental data (e.g., air pollution and meteorological data) with vegetation data (e.g., urban vegetation cover and leaf area data). The basic data used in this study are summarized in Table S1. Leaf Area Index (LAI) and evapotranspiration (ET) data were obtained from MODIS products, provided by NASA's Land Processes Distributed Active Archive Center (LP DAAC). MODIS LAI products are widely used in vegetation monitoring due to their high temporal and spatial resolution and continuous global coverage. Yan et al. (2021) evaluated the performance of MODIS and VIIRS LAI products across multiple years, demonstrating the stability of MODIS LAI products. On an urban scale, Imhoff et al. (2010) used MODIS LAI data to analyze the heat island effect in different urban biomes, showcasing the potential application of this dataset in urban microclimate studies. The spatial resolution of the LAI and ET data is 500 m, and the temporal resolution is 8 days. Daily LAI and ET values were estimated based on relative imagery over these eight days, assuming that LAI and ET values remained consistent within this period. To align with subsequent PM2.5 data, the LAI and ET data were resampled to a 1 km resolution in ArcGIS. As a preliminary assessment, using 1 km resolution data was intended to capture general trends and understanding over a large area. Although a 1 km resolution may have certain limitations in urban areas, it provides a macroscopic perspective that helps identify overall trends and patterns. Numerous related studies (Zhang et al., 2022; Gaglio et al., 2022; Shen et al., 2022; Yin et al., 2019) have shown that 1 km resolution data is feasible for using dry deposition models to study the PM2.5 removal by urban vegetation and can yield meaningful results.

 $PM_{2.5}$ data were obtained from the ChinaHighPM_{2.5} dataset (Geng et al., 2021; Xiao et al., 2022), a high-resolution, high-quality $PM_{2.5}$ dataset released by Dr. Wei Jing's team at the University of Maryland in 2021. This dataset integrates multiple satellite remote sensing sources and artificial intelligence technology, considering ground-based observations, satellite remote sensing products, atmospheric reanalysis, and emission inventories to address the spatiotemporal variability of air pollution. The deposition velocity and resuspension rate of $PM_{2.5}$ are related to wind speed. To improve the accuracy of deposition velocity parameters, we conducted experiments based on the indirect method proposed by Yin et al. (2019) using a smog chamber. The deposition velocity (V_d) was calculated using the following exponential decay model:

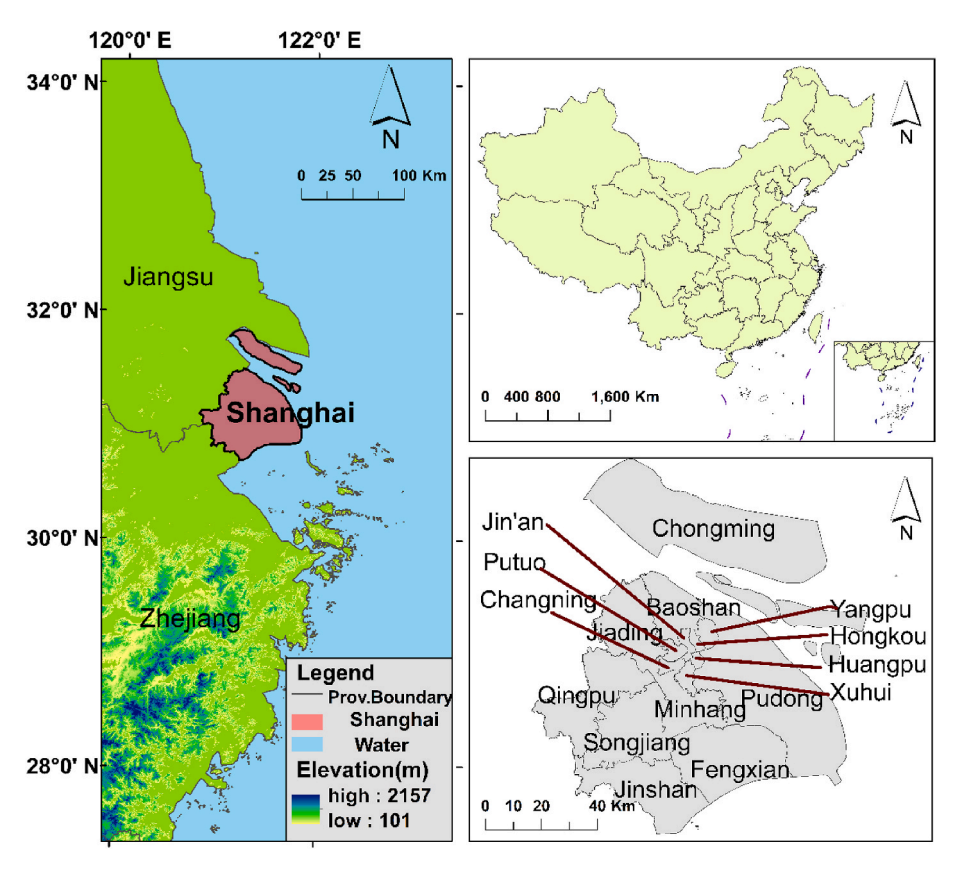


Fig. 1. Location of the study area.

$$V_d = \frac{V}{LA} \bullet \left(e^{-j \bullet \Delta t} - e^{-k \bullet \Delta t} \right) \tag{1}$$

where $V(m^3)$ is the volume of the smog chamber, LA (m^2) is the total leaf area, j and k are the decay rate constants under non-leaf and leaf conditions, respectively, and Δt is the time interval for concentration measurements (set to 1 s in this study). In this study, j and k and were determined through fitting the exponential decay curves under non-leaf and leaf conditions, respectively. The decay rate constant j was found to be 0.0009612 s^{-1} , while k varied by vegetation type. Representative local vegetation types were sampled, including Cinnamomum camphora, Ligustrum lucidum, Magnolia grandiflora, Sabina chinensis, Podocarpus macrophyllus, Cedrus deodara, Pinus parviflora, Metasequoia glyptostroboides, and various shrubs such as Euonymus japonicus 'Aureomarginatus', Rhaphiolepis indica, Photinia serratifolia, Ligustrum quihoui, Azalea, Ilex chinensis, and Pittosporum tobira. The results (Table S2) were further compared with deposition velocity data reported in other studies, particularly those conducted in Shanghai (Zhang et al., 2021; Liu et al., 2024). Our measurements for dense trees under wind speeds of $2-4 \text{ m} \cdot \text{s}^{-1}$ showed general alignment with Zhang et al. (2021), though slight deviations were observed at higher wind speeds, with differences within 15%. For shrubs, our measured deposition velocities were moderately higher (by approximately 8-12%) compared to Liu et al. (2024). These differences may be attributed to variations in experimental conditions and the selection of vegetation types. Despite these discrepancies, the overall trends of our measurements are comparable to existing studies in Shanghai, suggesting consistency within the regional context.

Meteorological data, including wind speed and precipitation, were collected from the National Meteorological Information Center. The data consists of 3-min interval records from 11 meteorological stations across Shanghai from January 2022 to December 2022. Shanghai's typical wind speed range is primarily between 0 and 6 $m \cdot s^{-1}$ (Ge et al.,

2001). Using Python, we extracted the 3-min wind speed and rainfall data for 2022 and applied kriging interpolation to generate daily meteorological element maps. Specifically, we employed co-kriging (Goovaerts, 2000), which incorporates elevation as a covariate to account for spatial variability. The kriging interpolation process was implemented using ArcMap 10.8. The semi-variogram model was selected as Gaussian, and the parameters (range, sill, nugget) were fitted to the data. The interpolation covered the spatial boundaries of Shanghai, and the resulting daily meteorological element maps were resampled to a 1 km unit size to match the subsequent raster calculations.

2.3. Local Climate Zone (LCZ) map

Local Climate Zones (LCZs) is a classification system used to describe urban and suburban surface cover characteristics and their impacts on local climate. This system was proposed by Stewart and Oke (2012), aiming to provide a standardized method for studying the effects of different urban environments on climate characteristics. LCZ divides the surface into various types, including different urban and natural surfaces, each classified based on its structure, materials, and thermal properties influenced by human activities.

Compared to traditional Land Use and Land Cover Classification (LUCC) methods, a major distinction of the LCZ approach is its focus on the impact of surface types on urban microclimate, rather than merely their physical and visible characteristics. While LUCC methods emphasize the biophysical attributes of the surface, such as vegetation cover and terrain, LCZ classifies based on climate-related properties like thermal capacity, thermal conductivity, and humidity. Moreover, LCZ incorporates surface height information, which is particularly important in urban environments, as building heights influence wind speed, air convection, and dry deposition. This results in different LCZ types having varying impacts on air flow and pollutant dispersion. Liu et al.

(2013) used remote sensing imagery to estimate the total above-ground vegetation biomass in different functional areas of Guangzhou and subsequently estimated the dust retention capacity of different functional areas and the city as a whole. Therefore, we selected the LCZ classification method to more accurately understand and quantify the specific impacts of urban surface characteristics on air quality. In this study, the classification of LCZ was performed using the World Urban Database and Access Portal Tools (WUDAPT) platform. The LCZ classification result (Fig. 2) for Shanghai in 2022 were obtained using the Random Forest classification algorithm and Landsat 8 data. The corresponding classification accuracy was evaluated and presented using box plots.

2.4. PM_{2.5} dry deposition model

To estimate the amount of PM_{2.5} removed by vegetation during non-precipitation periods in Shanghai in 2022, as well as the corresponding removal rates, we referred to the dry deposition module (UFORE-D) of the i-Tree model. The hourly pollutant removal flux $F_{i,j}$ ($\mu g \cdot m^{-2} \cdot h^{-1}$) for each pixel (area = 1 × 1 km) was calculated using the following equation:

$$F_{i,j} = V_{d,PM2.5} \cdot LAI_{i,j} \cdot C_{i,j} \cdot (1 - r_{i,j}) \times 3600$$
 (2)

The deposition velocity of PM_{2.5}, $V_{d,PM2.5}$ ($m \cdot s^{-1}$), represents the speed at which pollutants are deposited onto the leaf surface. This value is estimated based on literature and daily average wind speed. The term $\mathbf{r}_{i,j}$ represents the resuspension rate of PM_{2.5} on the leaves for the i th pixel on the j th day. The concentration of PM_{2.5}, $C_{i,j}$ ($\mu g \cdot m^{-3}$), is for the i th pixel on the j th day. The Leaf Area Index (LAI), LAI_{i,j} (m^2/m^2), for the i th pixel on the j th day, indicates the leaf area per unit ground area. The model coefficient 3600 adjusts the flux units to ($\mu g \cdot m^{-2} \cdot h^{-1}$) to facilitate subsequent analysis.

Based on the following formula, the annual removal rate $Q_i (\mu g \cdot m^{-2})$ at the pixel scale for urban vegetation can be estimated:

$$Q_{i} = \sum_{i=1}^{365} F_{ij} \cdot T_{ij} \tag{3}$$

The term T_{ij} represents the dry deposition time for pixel i on day j, which depends on the daily average precipitation. If the daily average precipitation exceeds $0.2 \times LAI_{ij}$ mm (Nowak et al., 2013), it is assumed that all particles are washed off the leaves, reducing the dry deposition time to zero. Otherwise, the dry deposition time is assumed to be 24 h.

To calculate the total amount of PM_{2.5} removed by urban vegetation in Shanghai in 2022, the removal rate Q_i is multiplied by the pixel area and then summed over the entire year. Here, n is the number of pixels, and A is the area of each pixel (1 × 1 km²):

$$Total PM_{2.5} removal = \sum_{i=1}^{n} Q_i \cdot A$$
 (4)

2.5. Seasonal and Trend Decomposition using Loess (STL)

In this study, we employed Seasonal and Trend Decomposition using Loess (STL) to analyze the temporal dynamics of vegetation's $PM_{2.5}$ removal capacity. STL decomposes a time series into three distinct components (Bandara et al., 2021; He et al., 2021): trend (T_t), seasonality (S_t), and residuals (R_t), represented as:

$$Y_t = T_t + S_t + R_t \tag{5}$$

where Y_t is the observed PM_{2.5} removal rate at time t, T_t reflects long-term trends, S_t captures periodic variations, and R_t represents short-term fluctuations or noise.

However, due to the complexity of $PM_{2.5}$ formation processes, particularly secondary and tertiary reactions, the residual component may contain uncaptured dynamic characteristics, potentially affecting the accuracy of the overall decomposition (Arangio et al., 2016). Additionally, STL's smoothing nature might attenuate extreme values, underestimating the impact of high-pollution events (Putrada et al., 2023). To address these limitations, we implemented modifications to

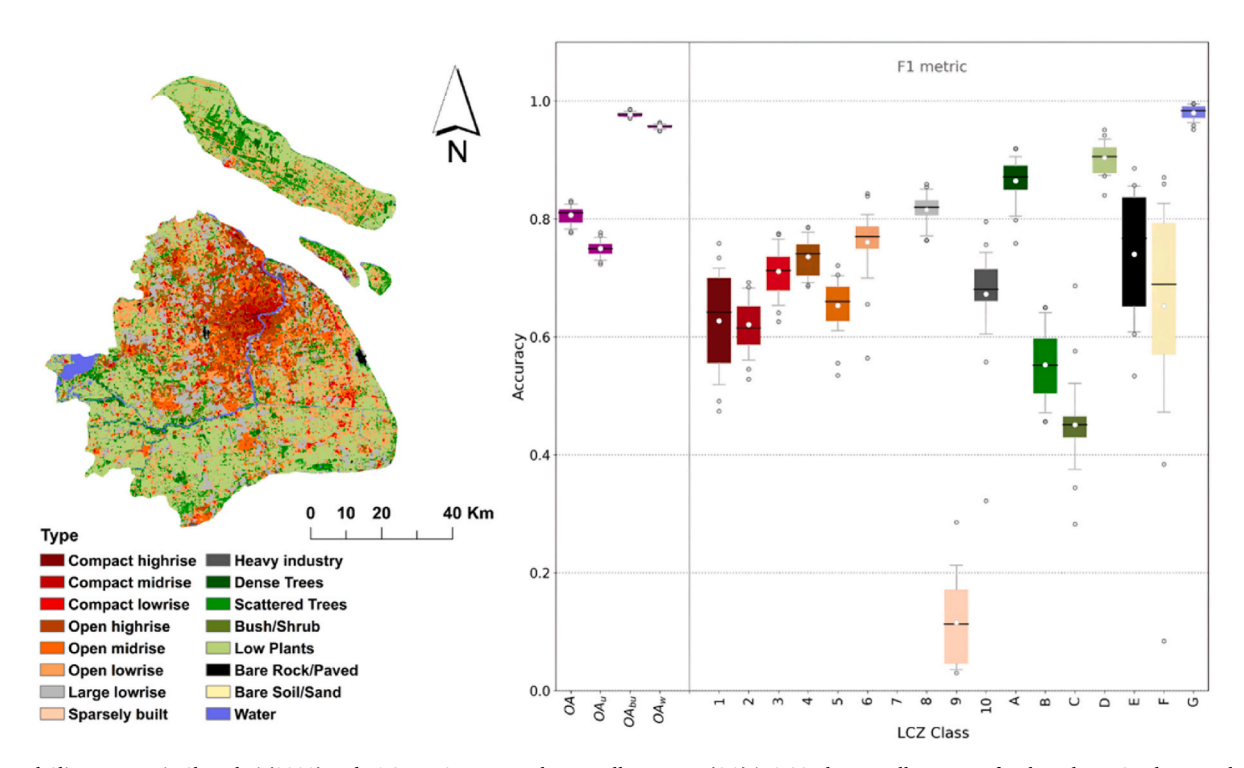


Fig. 2. Local Climate Zone in Shanghai (2022) and F1 Score Accuracy: The overall accuracy (OA) is 0.83, the overall accuracy for the urban LCZ classes only (OAu) is 0.76, the overall accuracy of the built versus natural LCZ classes only (OAbu) is 0.98, and the weighted accuracy (OAw) is 0.97.

the STL method. A random forest model was introduced to correct the original residuals (R_t), generating refined residuals (R_t^*) to better represent the dynamic characteristics. The correction is expressed as:

$$R_t^* = f(R_t) \tag{6}$$

where $f(\cdot)$ denotes the random forest model designed to learn and adjust for the residual's complex dynamics. Using the refined residuals, we updated the trend and seasonality components to ensure consistency with the corrected residuals. The updated formulas are:

$$T_t^* = Y_t - S_t - R_t^*, \quad S_t^* = Y_t - T_t^* - R_t^*$$
 (7)

These updates resulted in an optimized decomposition framework. The final decomposition model is expressed as:

$$Y_t = T_t^* + S_t^* + R_t^* \tag{8}$$

This improved method ensures that the decomposed components accurately represent the underlying data. The updated trend (T_{ϵ}^{*}) more accurately reflects long-term variations, the updated seasonality (S_t^*) better captures periodic fluctuations, and the refined residuals (R_t^*) incorporate dynamic features such as extreme events, improving the model's robustness. The STL analysis was implemented using Python, with daily PM2.5 removal rates as input data. To reduce short-term fluctuations and highlight long-term trends, a rolling window of 7 days was applied to smooth the data. This helped remove noise from short-term variations, making the underlying trend clearer. A Savitzky-Golay filter with a window size of 15 and a polynomial order of 3 was then applied to further smooth the data, effectively eliminating abrupt changes and small-scale noise. To capture seasonal patterns and variations linked to vegetation phenology and meteorological changes, a seasonal decomposition was performed using the STL method with a period of 30 days. The robust mode was enabled to mitigate the effects of outliers, enhancing the stability of the decomposition.

3. Results

3.1. Geospatial patterns of PM_{2.5} mitigation by urban vegetation

The 2022 forest resource monitoring results for Shanghai indicate that by the end of 2022, the city's forest coverage rate had reached 18.49%. Shanghai plans to increase the forest coverage rate to 23% by 2035. The majority of Shanghai's forests are concentrated in suburban areas, with suburban forests accounting for 97% and urban core areas accounting for 3%. The government departments of the nine suburban districts have all placed significant emphasis on afforestation and greening, exceeding the targets set for the 14th Five-Year Plan. Among these, Chongming District has made the largest contribution to the city's forest coverage rate by promoting the construction of a world-class ecoisland. The 2022 survey indicated that Chongming District's forest (including trees, bamboo, and special shrub forests) coverage rate had reached 30.05%.

In 2022, urban vegetation in Shanghai removed a total of 835 tons of PM_{2.5}, demonstrating its significant role in improving air quality. The PM_{2.5} removal flux averaged 0.51 \pm 0.03 g ·m $^{-2}$ ·year $^{-1}$, ranging from 0.08 to 1.12 g·m $^{-2}$. The PM_{2.5} removal rate varied across the city, with an average rate of 11.62 \pm 3.31%, a minimum of 4.09%, and a maximum rate of 21.7%.

Fig. 3 shows the spatial distribution estimate of $PM_{2.5}$ removal capacity $(g \cdot m^{-2})$ by vegetation in Shanghai for the year 2022. The $PM_{2.5}$ removal capacity of vegetation exhibits spatial heterogeneity, with a noticeable gradient change from the urban core to the suburban areas. The central urban area shows a lower $PM_{2.5}$ removal capacity, whereas certain suburban areas display higher removal rates. The regions with the highest $PM_{2.5}$ removal rates are concentrated in the western, southern, and Chongming Island areas of Shanghai, corresponding to

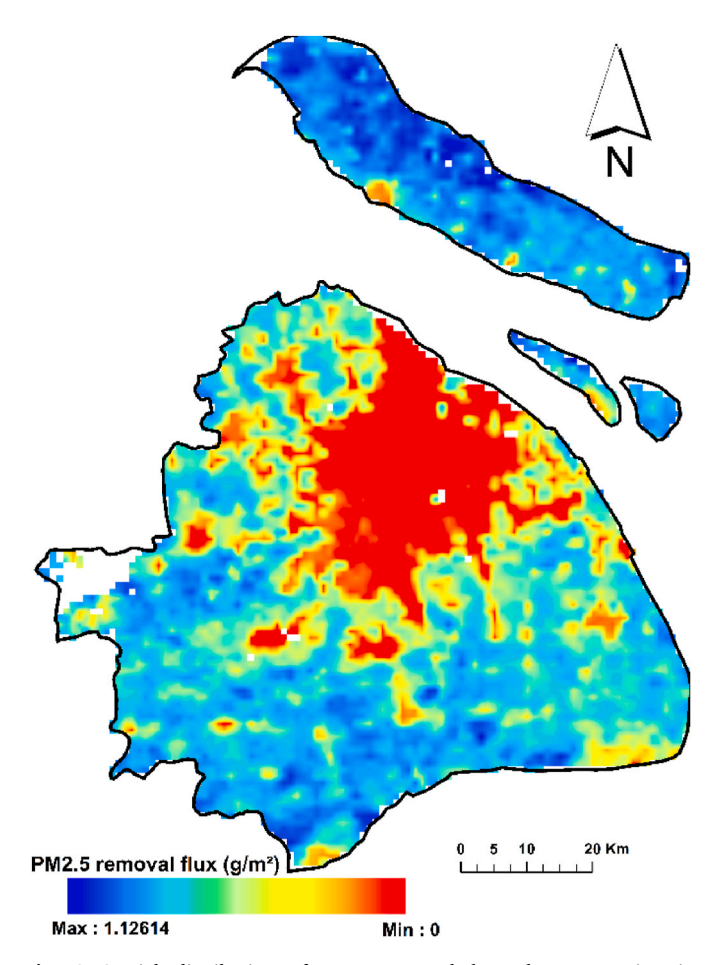


Fig. 3. Spatial distribution of $PM_{2.5}$ removal by urban vegetation in Shanghai City.

Qingpu District, Jinshan District, Fengxian District, and Chongming District, respectively. These areas have extensive green spaces. From the local climate zone map of Shanghai (Fig. 2), it can be seen that areas such as Yangpu District, Hongkou District, Jing'an District, Putuo District, Changning District, Xuhui District, Huangpu District, the waterfront of Pudong New Area along the Huangpu River, Baoshan District, and the southeastern part of Jiading District are mostly covered by midto high-rise buildings, with low vegetation density, resulting in significantly reduced $P\mathrm{M}_{2.5}$ removal amounts.

3.2. Contributions of the $PM_{2.5}$ removal capacity of LCZs

The results of this study reveal the differences in $PM_{2.5}$ removal capacities across various LCZs and their contributions to urban environmental purification. Among building land types, Open Lowrise has the largest area proportion, accounting for 17.35%. The three compact building types: Compact highrise, Compact midrise and Compact lowrise, accounting for 0.53%, 1.25%, and 2.82%, respectively. Large Lowrise is almost non-existent, with only 0.03% coverage (Table 1). Among all LCZ types, Dense Trees made the highest contribution to $PM_{2.5}$ removal, amounting to 208.28 tons. The green space type with the largest area, Bush/Shrub, followed closely with a removal amount of 194.81 tons.

Fig. 4 further illustrates these findings. Significance letters are added above the boxplots of different LCZ types, representing statistical groupings based on Tukey HSD test (p < 0.05). Groups sharing the same letter have no significant differences, while groups with different letters show significant differences. Detailed statistical results are provided in Table S4. The results show that Bush/Shrub, Compact lowrise, Large

Table 1 Distribution and PM_{2.5} mitigation contributions of LCZs.

LCZs	Area Percentage (%)	Area (km²)	Pollution Removal (tons)
1: Compact highrise	0.53	32.47	3.42
2: Compact midrise	1.25	76.69	4.07
3: Compact lowrise	2.82	173.10	22.79
4: Compact Open	9.00	553.12	41.17
highrise			
5: Open midrise	6.04	371.04	23.00
6: Open lowrise	17.35	1066.08	173.68
7: Lightweight lowrise	9.07	557.20	34.82
8: Large lowrise	0.03	1.74	0.65
9: Sparsely built	0.67	41.04	5.51
10: Heavy industry	1.73	106.08	55.49
11: Dense Trees	10.01	615.22	208.28
12: Scattered Trees	1.63	100.32	63.42
13: Bush/Shrub	36.50	2242.32	194.81
14: Low Plants	0.43	26.31	4.14

Note: "Bare Rock/Soil" and "Water" are not included in the statistics.

lowrise, and Scattered Trees have no significant differences in PM25 removal rates (sharing letter "a"), whereas Dense Trees, Heavy industry, and other built-up types (such as Compact highrise and Compact midrise) exhibit significant differences. Overall, vegetated types, such as Dense Trees and Bush/Shrub, demonstrate more stable PM_{2.5} removal rates and significantly higher removal rates compared to some built-up types. In contrast, Large lowrise shows greater variability in removal rates due to differences in building height and density. Notably, the heavy industrial areas exhibit the highest removal efficiency. Many studies agree that vegetation effectively captures and adsorbs airborne particulates, thus reducing $PM_{2.5}$ concentrations. However, the dust retention capacity of vegetation is limited (Sun et al., 2020; Liu et al., 2013). When PM_{2.5} concentrations are excessively high, the adsorption capacity of vegetation becomes saturated (Wróblewska et al., 2021), and the dry deposition model does not account for this limitation. This explains why heavy industrial areas have the highest removal efficiency. Nonetheless, this high efficiency does not imply that vegetation can maintain high removal efficiency in such areas over the long term.

Instead, the dust retention capacity of vegetation quickly decreases under high pollution conditions, necessitating frequent vegetation replacement, tree gardening to maintain plant health, leaf washing to remove accumulated dust, and adding trees to enhance vegetation coverage. Excluding the impact of PM_{2.5} concentration by heavy industrial activities, the order of removal efficiency should be Dense Trees > Open low-rise > Large low-rise > Bush/Shrub > Scattered Trees > Others.

3.3. Temporal dynamics of PM_{2.5} mitigation trends

To explore the temporal variation and seasonal differences in PM_{2.5} removal flux, we applied Seasonal and Trend decomposition using Loess (STL) to the original removal sequence. As shown in Fig. 5, the original series was decomposed into trend, seasonal, and residual components. The trend plot reveals the long-term changes in the data and highlights a "double peak" pattern: the removal flux begins to rise rapidly in March and April following the winter season, followed by a brief decline after spring. Another rise starts in July, peaking in August. To validate the statistical significance of the double peak pattern, we employed two complementary statistical methods. The t-test, a parametric test, evaluates whether the mean PM2.5 removal flux during the double peak periods differs significantly from that during other periods under the assumption of normality. The Mann-Whitney U test, a non-parametric alternative, assesses whether the distributions of the two groups differ without assuming normality. Both methods confirmed that the PM_{2.5} removal flux during the double peak periods was significantly higher than that of other periods, with p < 0.001. These statistical results are displayed in Fig. 5, alongside the marked positions of the double peaks, to provide a clear and rigorous validation of the observed pattern.

The $PM_{2.5}$ removal flux exhibits significant fluctuations within certain months (e.g., May and September), while it remains relatively stable in other months (e.g., February and July) as shown in Fig. 6a. The violin plots for January to April (transition from winter to spring) display a wide bottom, particularly in February and March, indicating many low flux values during these months. The violin plots for May and June (late spring to early summer) are wider, especially above the median, indicating better $PM_{2.5}$ removal performance during this period.

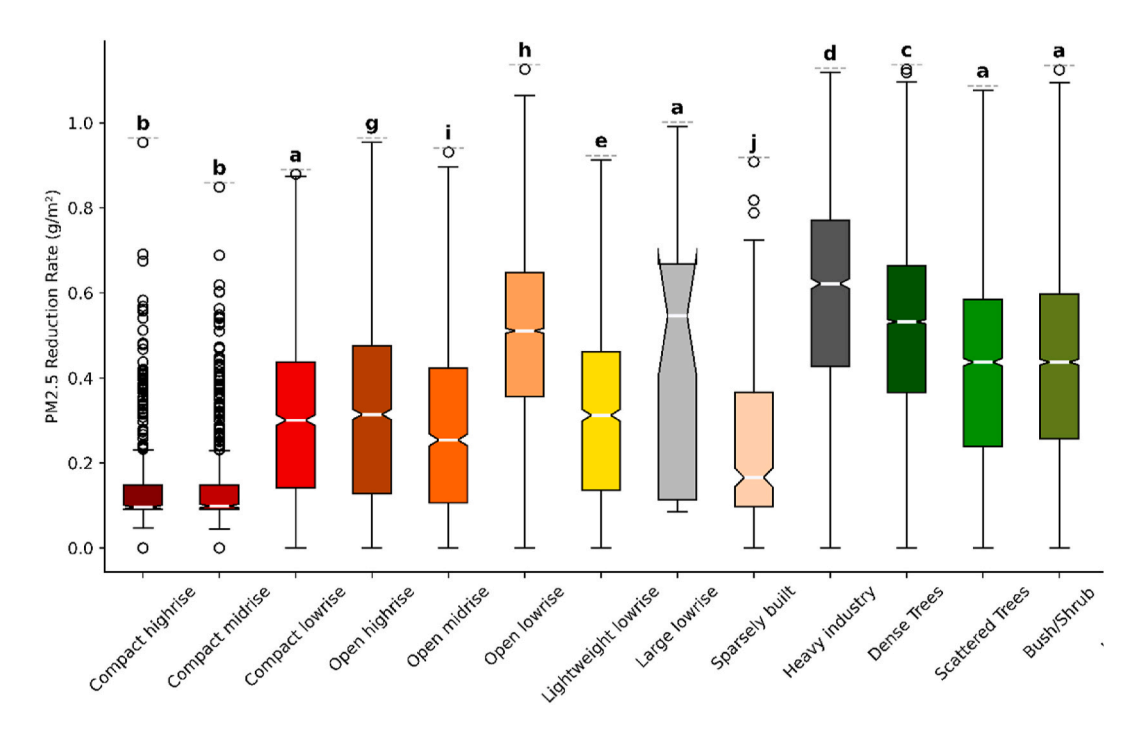


Fig. 4. PM_{2.5} mitigation across LCZs: distribution patterns of mitigation effectiveness. Letters above boxes indicate statistical groupings based on Tukey HSD test (*p* < 0.05). Groups sharing the same letter are not significantly different.

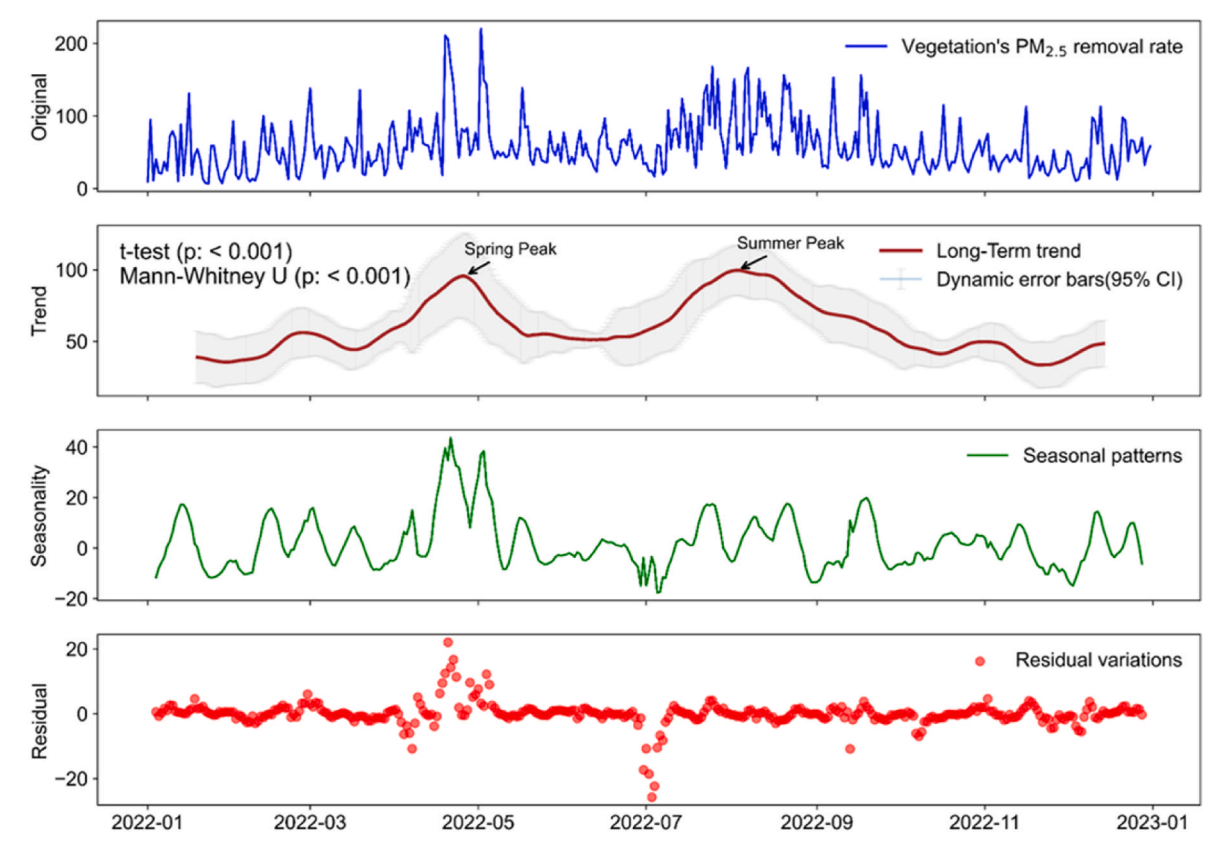


Fig. 5. Time series of PM_{2.5} removal rate from vegetation, decomposed into trend, seasonal patterns, and residuals using STL. The trend shows a significant increase during spring and summer peaks. Statistical significance was tested using t-test and Mann-Whitney U test (p < 0.001).

Furthermore, Fig. 6b shows that high removal windows are concentrated in April–May and July–August, with an average removal flux of 71.6 $\mu g\ m^2 \cdot h^{-1}$. During summer, the vigorous growth of vegetation, along with strong photosynthesis and transpiration, significantly enhances $PM_{2.5}$ removal, resulting in a higher average removal flux. In contrast, the removal effectiveness is weaker in autumn and winter, with average removal fluxes of 49.07 $\mu g\ m^2 \cdot h^{-1}$ and 44.80 $\mu g\ m^2 \cdot h^{-1}$, respectively (Fig. 6d). Fig. 6c illustrates the broad fluctuations in removal flux during spring and autumn, whereas summer displays a more concentrated distribution. Winter values show a relatively wide distribution, particularly around the median, indicating a higher variability in $PM_{2.5}$ removal effectiveness by vegetation during the winter season.

3.4. Impact of evapotranspiration on $PM_{2.5}$ reduction

Fig. 7a illustrates the relationship between evapotranspiration and the $PM_{2.5}$ reduction rate, with error ellipses (3 standard deviations) used to show the data distribution. The ellipses clearly reflect the concentration trend of the data, with point density decreasing as it moves further from the center. The red dot represents the mean value. In the error ellipse chart, the more elongated the ellipse, the stronger the correlation, and the tilt direction indicates the correlation direction. The rightward tilt of the ellipse suggests a positive correlation between the two variables, where an increase in evapotranspiration corresponds with an increase in the $PM_{2.5}$ reduction rate. Regression analysis between evapotranspiration and the reduction rate shows a moderate correlation, with an r of 0.52 and an R^2 of 0.28. This relatively low R^2 is primarily due to the study's focus on the singular effect of evapotranspiration on $PM_{2.5}$ reduction, without considering other potential environmental variables.

Despite the low R^2 , the correlation between evapotranspiration and

 $PM_{2.5}$ reduction remains significant, with a p less than 0.01, indicating statistical significance. To further investigate the nuanced effects of evapotranspiration on PM2.5 removal, this study employed an equalinterval division method to divide evapotranspiration into five intervals, capturing the variation in PM2.5 reduction across different evapotranspiration levels. The specific ranges for each interval are: Q1 (16.39 mm-38.20 mm), Q2 (38.20 mm-42.68 mm), Q3 (42.68 mm-46.59 mm), Q4 (46.59 mm-50.64 mm), and Q5 (50.64 mm-73.99 mm). From the density distribution plot in Fig. 7b, a complex relationship between evapotranspiration and PM_{2.5} reduction can be observed. The high-density region is concentrated in the medium evapotranspiration range (38 mm-50mm), with a PM_{2.5} reduction rate around 0.6 $g \cdot m^{-2}$, indicating that removal efficiency is both significant and stable in this range. In contrast, data points in the lower (<38 mm) and higher (>50 mm) evapotranspiration ranges are more scattered, with reduced density, suggesting greater variability in removal efficiency and some degree of uncertainty.

To more accurately assess the changes in removal efficiency across different evapotranspiration intervals, we calculated the marginal effect for each interval by computing the mean $PM_{2.5}$ reduction rate and the differences between adjacent intervals (Table 2). The marginal effect was highest in the Q2 interval (38.20 mm–42.68 mm), reaching 0.67, indicating that the increase in evapotranspiration had the most significant effect on $PM_{2.5}$ reduction within this range. However, as evapotranspiration increased further, the marginal effect gradually declined in the Q3 to Q4 intervals (42.68 mm–50.64 mm), dropping to 0.17 and 0.09, respectively, showing a slowing rate of improvement in removal efficiency. In the Q5 interval (50.64 mm–73.99 mm), the marginal effect slightly rebounded to 0.28, suggesting that other environmental factors may have contributed to the $PM_{2.5}$ removal efficiency under higher evapotranspiration conditions. This could be related to stomatal regulation, where stomata begin to close as evapotranspiration exceeds a

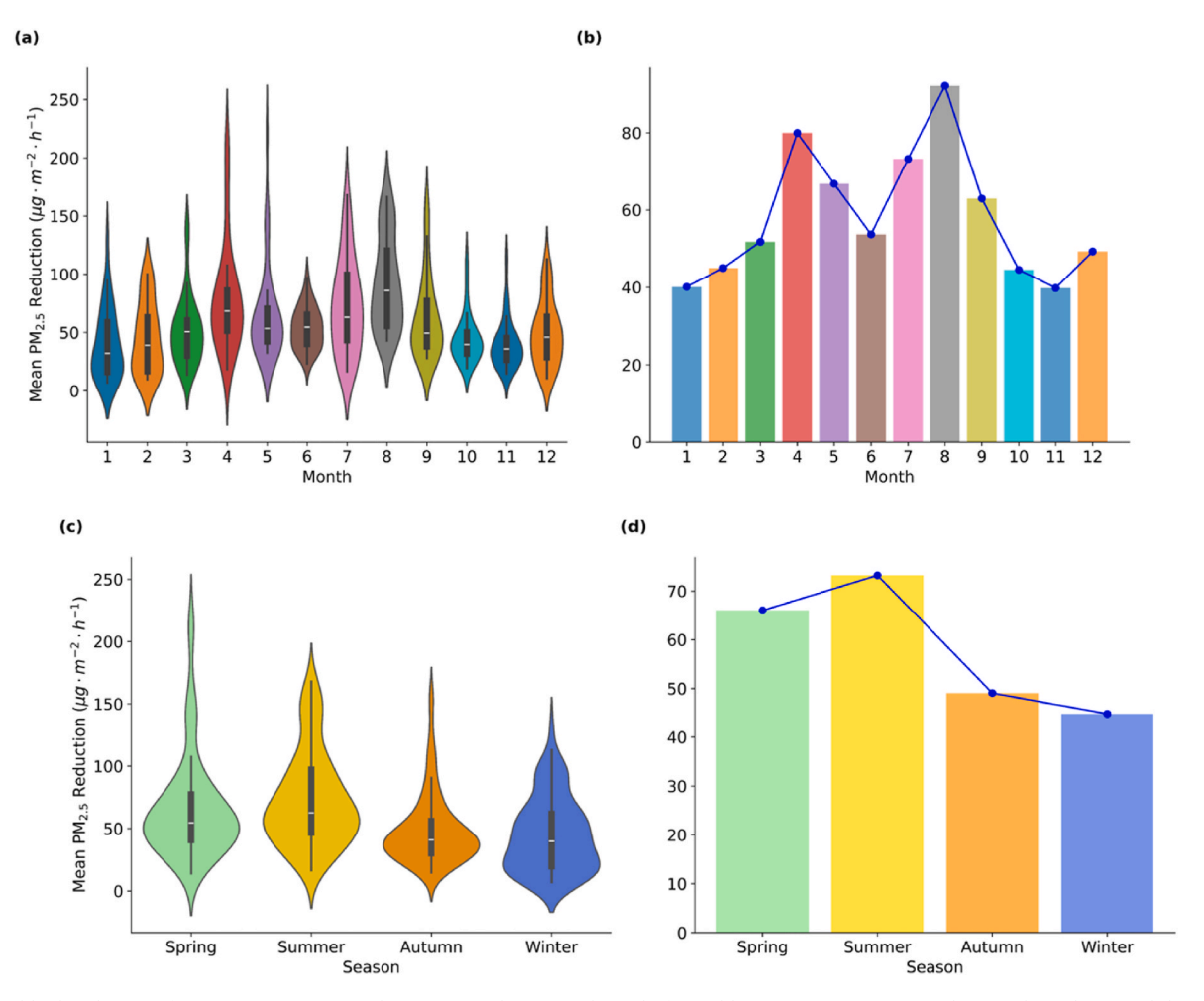


Fig. 6. Monthly distribution of $PM_{2.5}$ concentration reduction (a) and mean and trend of monthly $PM_{2.5}$ concentration reduction (b) and seasonal distribution of $PM_{2.5}$ concentration reduction (c) and mean and trend of seasonal $PM_{2.5}$ concentration reduction (d).

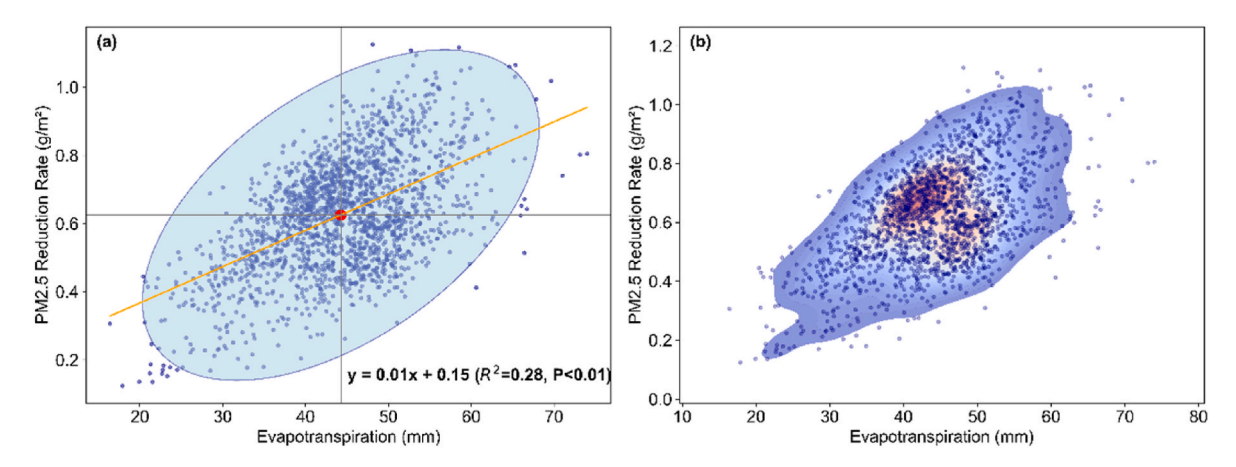


Fig. 7. The positive correlation between evapotranspiration and $PM_{2.5}$ reduction is illustrated in (a), while (b) shows the density distribution, highlighting the concentration of reduction at moderate evapotranspiration levels.

certain threshold, reducing particle capture efficiency. However, under certain environmental conditions, factors such as humidity or stomatal mechanisms may enhance removal efficiency once again.

4. Discussion

4.1. PM_{2.5} removal and spatiotemporal variation

Our study estimates the removal of PM_{2.5} by urban vegetation in Shanghai using the UFORE-D module, with a total annual removal of 835 tons and an average rate of 0.51 $g \cdot m^{-2} \cdot year^{-1}$. In a field study conducted by Su et al. (2020) in Taiwan, similar results were obtained.

Table 2 Evapotranspiration and $PM_{2.5}$ reduction, showing mean reduction, standard deviation, and marginal effect for each interval.

Evapotranspiration interval	Mean PM _{2.5} reduction $(g \cdot m^{-2})$	Standard deviation	Marginal effect
Q1 (16.39 mm–38.20 mm)	0.487970	0.141595	-
Q2 (38.20 mm-42.68 mm)	0.612881	0.122199	0.667848
Q3 (42.68 mm-46.59 mm)	0.642798	0.133918	0.165023
Q4 (46.59 mm–50.64 mm)	0.660048	0.148857	0.086149
Q5 (50.64 mm–73.99 mm)	0.722282	0.160557	0.284249

They validated the i-Tree Eco model estimates through on-site mobile monitoring and found that the PM_{2.5} removal rates by vegetation ranged from 2.51% to 35.57%, demonstrating the reliability of the UFORE-D module in estimating PM_{2.5} removal. Liu et al. (2020) used the UFORE-D dry deposition module and GeoDetector to estimate the spatiotemporal patterns in the Fenwei Plain of China. Their results showed that the average PM_{2.5} removal rates by vegetation in 2000, 2010, and 2021 were 0.186%, 0.243%, and 0.435%, respectively, which are similar to the findings of this study. In Shanghai, a study by Zhang et al. (2021) estimated that urban forests removed approximately 874 tons of PM_{2.5} in 2017, which is comparable to the 835 tons estimated in this study for 2022. The observed differences may be attributed to variations in vegetation coverage and meteorological conditions between the two time periods. Additionally, the study highlighted seasonal variability, with the highest PM2.5 removal in summer, and spatial variability, where suburban areas contributed more significantly than urban centers. These seasonal and spatial patterns are consistent with the trends observed in this study.

Vegetation has a significant mitigating effect on air pollution, as confirmed by many studies (Dwijendra et al., 2023; Zhai et al., 2022). These effects of vegetation have been evaluated using a variety of models and methods, each with distinct assumptions and applicable scales. The UFORE module is widely used for quantifying urban vegetation's ecosystem services due to its computational efficiency and relatively simple parameterization, making it suitable for large-scale assessments (Nowak et al., 2013). However, it simplifies certain processes, such as assuming uniform deposition velocities and leaf area index, which may not fully reflect the complexity of deposition dynamics in heterogeneous urban environments. The current limitation of the model's resolution primarily comes from the wind speed data. Wind speed is a key factor influencing the model's core parameter, deposition velocity, especially in densely built urban areas where the layout of streets and buildings significantly affects airflow. Finer-resolution wind speed data can more accurately reflect local airflow patterns, particularly in areas with dense buildings and complex street layouts, thereby improving the estimation of deposition velocity and further optimizing the assessment of PM_{2.5} removal capacity. Meanwhile, increasing the spatial resolution of the Leaf Area Index (LAI) data can also significantly improve the model's accuracy. Higher-resolution LAI data can more precisely depict vegetation coverage in different urban areas, particularly in regions with complex green space distribution or limited greenery, allowing the model to more accurately evaluate the contribution of various green spaces to PM2.5 removal. In contrast, the ENVI-met model provides high-resolution simulations by incorporating detailed microclimatic processes, such as wind speed, temperature, and pollutant dispersion, which are particularly effective for small-scale studies (Bruse and Fleer, 1998). Yet, its high computational cost often restricts its application to limited areas. To address this limitation, future research could integrate the strengths of both models by combining ENVI-met's microclimatic simulations with i-Tree Eco's

ecological benefit calculations. Specifically, microclimate data generated by ENVI-met, including wind speed, temperature variations, and pollutant concentrations, can be used as input to optimize i-Tree Eco's parameters, particularly in environments with complex urban layouts and dynamic weather conditions. This integration would enhance the accuracy of ecological assessments, such as particulate matter retention and overall air quality improvement, by providing a more nuanced understanding of how vegetation interacts with its environment. Additionally, combining these models would enable cross-scale analyses, from small-scale simulations of individual parks or street canyons to large-scale urban green space planning, offering a more comprehensive and scalable approach to urban vegetation management. This combined framework would allow for a more precise evaluation of the spatial and temporal dynamics of vegetation's role in mitigating urban environmental challenges, such as air pollution and heat island effects.

Fig. 5 illustrates the seasonal dynamics of vegetation's PM_{2.5} removal flux, characterized by a distinct double-peak pattern in spring and summer. These seasonal variations are primarily influenced by a combination of vegetation activity and atmospheric conditions. In spring (March to April), the first peak coincides with the rapid recovery of vegetation coverage. The increased surface area significantly enhances the interception and dry deposition of particles, leading to a marked rise in removal flux. Additionally, the elevated relative humidity during spring enhances the hygroscopic growth of particles, facilitating their deposition on vegetation surfaces. This phenomenon has been demonstrated in studies of Shanghai, where humid conditions significantly promote PM2.5 removal, providing a reasonable explanation for the spring peak (Liu et al., 2018). The second peak in summer (July to August) aligns with the annual maximum vegetation coverage, offering an expanded surface area for particle deposition. Concurrently, elevated temperatures and strong convective conditions result in higher particle concentrations in the atmosphere, particularly due to the intensified formation of secondary particles such as nitrates and sulfates. This process, driven by accelerated photochemical reactions, creates favorable conditions for vegetation to capture these particles (Qiao et al., 2014). However, this double-peak pattern also highlights the temporal mismatch between vegetation's removal capacity and PM_{2.5} emissions. Winter represents the period of highest PM_{2.5} concentrations (Xiao et al., 2015), primarily driven by emissions from northern heating activities, while vegetation coverage and activity are significantly reduced during this time, resulting in a noticeable decline in filtering capacity.

4.2. Role of evapotranspiration in enhancing $PM_{2.5}$ mitigation

Previous studies have shown that various environmental factors influence leaf dust retention and the pollution removal efficiency of vegetation (Li et al., 2023b). Precipitation significantly enhances PM2.5 removal efficiency by washing particles off leaves and reducing the chance of resuspension, particularly during high-rainfall periods. Wind speed also plays a crucial role by facilitating particle deposition and increasing air exchange near leaf surfaces, which enhances the effectiveness of vegetation in capturing PM_{2.5} (Pace & Grote, 2020). Beyond precipitation and wind, other meteorological factors such as temperature, humidity, and atmospheric pressure have been found to significantly impact PM2.5 concentrations. For instance, increased humidity raises leaf surface wetness, promoting particle adhesion, while high temperatures accelerate evapotranspiration, indirectly improving particle retention (Yan et al., 2020; Zhang et al., 2016). Furthermore, the combined effects of meteorological factors often exhibit nonlinear and lagged relationships. For example, the influence of rainfall and wind on PM_{2.5} reduction may persist for several days, while humidity and temperature effects often peak rapidly before diminishing (Yang et al., 2021). These interactions highlight the complexity of environmental influences on PM_{2.5} removal. This study focuses on evapotranspiration as a central mechanism, given its direct role in regulating leaf-atmosphere interactions and its potential to interact with other

meteorological factors to enhance particle retention (Chen et al., 2020; Han et al., 2020).

Our experiment also found that while there is a significant positive correlation between evapotranspiration and removal efficiency, changes in evapotranspiration do not always align with changes in PM2.5 removal rates. In the moderate evapotranspiration range (40-50 mm), removal efficiency reached a relatively high and stable level (Fig. 7b), indicating that evapotranspiration has the most pronounced effect on PM_{2.5} removal within this range. By significantly increasing local atmospheric humidity, evapotranspiration creates favorable conditions for the hygroscopic growth of fine particles. Higher humidity enlarges particle diameter and enhances deposition velocity, facilitating their deposition onto leaf surfaces. This humidity effect not only optimizes particle capture conditions around vegetation but also becomes particularly pronounced in high-humidity environments (Ebrahimian et al., 2019). At the same time, evapotranspiration directly influences particle capture through stomatal regulation. Under moderate evapotranspiration, stomata remain open, enhancing particle deposition efficiency. However, when evapotranspiration exceeds a certain threshold, plants may partially or completely close their stomata to maintain water balance, reducing further particle capture (Kool et al., 2014). Studies have demonstrated that changes in stomatal conductance play a critical role in determining the contribution of evapotranspiration to particle capture (Rosenberg et al., 1989), further highlighting the importance of stomatal dynamics in this process. Additionally, evapotranspiration significantly impacts particle transport efficiency by altering aerodynamic conditions around leaf surfaces. By reducing boundary layer thickness, evapotranspiration lowers resistance to particle transport, enhancing deposition efficiency. This boundary layer dynamic is particularly critical in low-wind-speed environments, where evapotranspiration improves local airflow exchange and creates more favorable conditions for particle capture (Cascone et al., 2019). However, as evapotranspiration increased, the improvement in removal efficiency diminished, showing a clear marginal effect. In the 42-50 mm range, the effect weakened noticeably, and beyond 50 mm, this decline became more pronounced. This trend suggests that excessive evapotranspiration leads to a saturation point, beyond which further increases do not significantly enhance removal efficiency. This may be due to stomatal behavior, as excessive evapotranspiration reduces the vapor pressure deficit (Xu et al., 2016), prompting stomata to partially or completely close, thereby limiting PM_{2.5} capture efficiency.

4.3. Implications and uncertainties

This study quantitatively estimated the capacity of urban vegetation to remove $PM_{2.5}$, emphasizing its key role in improving urban air quality. Using Shanghai as a case study, the i-Tree Eco model was applied to assess vegetation's $PM_{2.5}$ removal capacity across different periods and Local Climate Zones (LCZs) in 2022. Results showed that vegetation reduces $PM_{2.5}$ through dry deposition, and evapotranspiration significantly enhances removal efficiency. However, this effect diminishes beyond 50 mm. These findings not only contribute to a comprehensive understanding of the role of vegetation in air pollution control but also offer specific guidance for the development and management of future urban green infrastructure. Despite the achievements of this study, there are still several limitations that need to be addressed in future research.

First, model limitations are a key issue. While this study employs the i-Tree Eco model to estimate $PM_{2.5}$ removal by urban vegetation, we acknowledge its limitations in capturing the detailed effects of urban micro-scale features, such as varying building heights, street canyon effects, and local airflow dynamics. These micro-scale processes can influence $PM_{2.5}$ transport and deposition but are beyond the spatial resolution and functional scope of the i-Tree Eco model. To complement this limitation, micro-scale models such as ENVI-met offer an alternative approach for simulating detailed urban environments. ENVI-met

integrates three-dimensional airflow, pollutant dispersion, and vegetation interactions, making it suitable for small-scale studies, such as street-level analysis. However, due to its high computational cost and focus on localized areas, ENVI-met is not ideal for large-scale regional assessments, which remain the primary strength of i-Tree Eco. Future studies could explore combining both approaches: using i-Tree Eco for regional-scale evaluations and ENVI-met for micro-scale refinements to achieve a more comprehensive understanding of vegetation's role in mitigating PM_{2.5} pollution across different spatial scales. Second, this study does not explicitly account for the vertical distribution of PM_{2.5}, which represents a limitation. Existing studies on vertical distribution often rely on atmospheric models (e.g., WRF-Chem) or lidar-based observations. While these methods excel at simulating vertical variations, their computational complexity and data requirements have limited their widespread application in large-scale urban vegetation studies. The PM_{2.5} data used in this study primarily represent surface-level concentrations, which are suitable for large-scale analysis. However, vertical variations may influence deposition velocities and removal capacity. Future research should incorporate high-resolution vertical profiles or multilayer atmospheric models to further enhance the accuracy of PM_{2.5} removal estimates by urban vegetation. Finally, we did not sufficiently account for the seasonal variation in vegetation characteristics, particularly how the growth and senescence cycles of plants (such as leaf emergence, maturation, and leaf drop) may influence their particulate matter (PM) removal capabilities. The growth and maturation of leaves during the spring and summer seasons likely enhance the plant's ability to capture and retain particulate matter due to increased leaf area and more active photosynthesis. However, during the fall and winter seasons, as plants enter dormancy and lose their leaves, the PM removal efficiency of vegetation may decrease significantly. Previous studies have shown that plant foliage in active growth phases is more effective at trapping particulate matter, while the reduction in leaf area during the autumn and winter leads to diminished removal efficiency (Wang et al., 2013). Additionally, the leaf surface characteristics, such as waxy coatings, change with the seasons, further influencing the plant's ability to capture particulates. Due to the scope of this study and its limited temporal design, we were unable to fully assess the potential impact of seasonal changes in vegetation characteristics on particulate matter removal. Future research could incorporate seasonal variations into the analysis framework to more accurately evaluate the role of vegetation in air purification throughout the year, further enhancing our understanding of its contribution to improving urban air quality.

5. Conclusions

This study aimed to assess the removal effect of urban vegetation on PM_{2.5} by combining ground station data with remote sensing data and using the i-Tree model for dry deposition estimation. Based on the basic removal effects obtained, the contributions of different LCZ types were statistically analyzed. The study examined the variation in removal flux throughout the year and its seasonal characteristics, and explored the impact of surface evapotranspiration on the PM2.5 removal by vegetation. The results estimate that urban vegetation significantly reduces PM_{2.5}, with a total removal of 835 tons in 2022, an average removal rate of 0.51 g $\cdot m^{-2} \cdot year^{-1}$ per unit leaf area, and an average air quality improvement of 4.07%. Different LCZ types contributed differently to the removal amount, with Dense Trees > Open Lowrise > Large Lowrise > Bush/Shrub > Scattered Trees > Others. Considering both removal amount and rate, Open Lowrise demonstrated significant dust retention potential among the surface types. Its low building density and ample open spaces provide an optimal environment for dust retention processes. Additionally, the PM_{2.5} removal flux by vegetation exhibited a "double peak" pattern, with a rapid increase in removal flux observed in March and April after winter, a brief decline after spring, another rise starting in July, and a peak in August. The removal flux also displayed clear seasonal characteristics, with higher fluxes in spring and summer and lower fluxes in winter. By analyzing the relationship between evapotranspiration and $PM_{2.5}$ removal rate, we found that an increase in evapotranspiration significantly enhances the $PM_{2.5}$ purification effect of vegetation. However, this improvement does not continue to rise with further increases in evapotranspiration.

CRediT authorship contribution statement

Wei Yang: Writing – review & editing, Writing – original draft, Methodology, Formal analysis, Data curation, Conceptualization. Wenpeng Lin: Supervision, Project administration. Yue Li: Writing – original draft, Data curation. Yiwen Shi: Visualization, Investigation. Yi Xiong: Resources.

Declaration of competing interest

The authors declare that they have no known competing financial interests or personal relationships that could have appeared to influence the work reported in this paper.

Appendix A. Supplementary data

Supplementary data to this article can be found online at https://doi.org/10.1016/j.envpol.2025.125800.

Data availability

Data will be made available on request.

References

- Abhijith, K., Kumar, P., 2020. Quantifying particulate matter reduction and their deposition on the leaves of green infrastructure. Environ. Pollut. 265 (Pt B), 114884.
- Altimir, N., Tuovinen, J., Vesala, T., Kulmala, M., Hari, P., 2004. Measurements of ozone removal by Scots pine shoots: calibration of a stomatal uptake model including the non-stomatal component. Atmos. Environ. 38, 2387–2398.
- Arangio, A., Tong, H., Socorro, J., Pöschl, U., Shiraiwa, M., 2016. Quantification of environmentally persistent free radicals and reactive oxygen species in atmospheric aerosol particles. Atmos. Chem. Phys. 16, 13105–13119.
- Bandara, K., Hyndman, R., Bergmeir, C., 2021. MSTL: a seasonal-trend decomposition algorithm for time series with multiple seasonal patterns. Int. J. Oper. Res.
- Bruse, M., Fleer, H., 1998. Simulating surface-plant-air interactions inside urban environments with a three-dimensional numerical model. Environ. Model. Software 13 (3/4), 373–384.
- Cascone, S., Coma, J., Gagliano, A., Pérez, G., 2019. The evapotranspiration process in green roofs: a review. Build. Environ.
- Chen, Z., Chen, D., Zhao, C., Kwan, M., Cai, J., Zhuang, Y., Zhao, B., Wang, X., Chen, B., Yang, J., Li, R., He, B., Gao, B., Wang, K., Xu, B., 2020. Influence of meteorological conditions on PM2.5 concentrations across China: a review of methodology and mechanism. Environ. Int. 139, 105558.
- Choi, Y., Song, H., Jo, J., Bang, S., Park, B., Kim, H., Kim, K., Jeong, N., Kim, J., Kim, H., 2021. Morphological and chemical evaluations of leaf surface on particulate Matter 2.5 (PM 2.5) removal in a botanical plant-based biofilter system. Plants 10.
- Corada, K., Woodward, H., Alaraj, H., Collins, C., 2020. A systematic review of the leaf traits considered to contribute to removal of airborne particulate matter pollution in urban areas. Environ. Pollut., 116104
- Du, J., Zhang, X., Huang, T., Gao, H., Mo, J., Mao, X., J, 2019. Removal of PM2.5 and secondary inorganic aerosols in the North China Plain by dry deposition. Sci. Total Environ. 651 (Pt 2), 2312–2322.
- Dwijendra, N., Mohammadi, M., Aravindhan, S., Jalil, A., Taherian, M., Iswanto, A., Ekrami, H., Alborzi, M., Mousavion, K., 2023. Investigating the effects of air pollution on plant species resistance in urban areas. Health Scope.
- Ebrahimian, A., Wadzuk, B., Traver, R., 2019. Evapotranspiration in green stormwater infrastructure systems. Sci. Total Environ. 688, 797–810.
- Feng, S., Gao, D., Liao, F., Zhou, F., Wang, X., 2016. The health effects of ambient PM2.5
 and potential mechanisms. Ecotoxicology and environmental safety 128, 67–74.
 Gaglio, M., Pace, R., Muresan, A.N., Grote, R., 2022. Species-specific efficiency in PM2.5
- removal by urban trees: from leaf measurements to improved modeling estimates. Sci. Total Environ.
- Ge, Y., Xiang, H., 2001. Statistical study for mean wind velocity in Shanghai area. Journal of Web Engineering 89, 409–412.
- Geng, G., Xiao, Q., Liu, S., Liu, X., Cheng, J., Zheng, Y., Xue, T., Tong, D., Zheng, B., Peng, Y., Huang, X., He, K., Zhang, Q., 2021. Tracking air pollution in China: near real-time PM2.5 retrievals from multisource data fusion. Environ. Sci. Technol. 55, 12106–12115.
- Goovaerts, P., 2000. Geostatistical approaches for incorporating elevation into the spatial interpolation of rainfall. J. Hydrol. 228, 113–129.

- Han, D., Shen, H., Duan, W., Chen, L., 2020. A review on particulate matter removal capacity by urban forests at different scales. Urban For. Urban Green. 48, 126565.
- He, H., Gao, S., Jin, T., Sato, S., Zhang, X., 2021. A seasonal-trend decomposition-based dendritic neuron model for financial time series prediction. Appl. Soft Comput. 108, 107488
- He, B., Yu, G., Zhang, X., He, Z., Wang, Q., Liu, Q., Mao, J., Zhang, Y., 2022. Contributions of regional transport versus local emissions and their retention effects during PM2.5 pollution under various stable weather in Shanghai. Front. Environ. Sci. 10
- Huang, W., 2023. Impacts of PM2.5 on stock's earnings in China. International Journal of Information Systems and Informatics.
- Imhoff, M.L., Zhang, P., Wolfe, R.E., Bounoua, L., 2010. Remote sensing of the urban heat island effect across biomes in the continental USA. Rem. Sens. Environ. 114 (3), 504–513.
- Jeanjean, A.P.R., Monks, P.S., Leigh, R.J., 2016. Modelling the effectiveness of urban trees and grass on PM2.5 reduction via dispersion and deposition at a city scale. Atmos. Environ. 147, 1–10.
- Jeong, N., Han, S., Ko, B., 2023. Effects of green network management of urban street trees on airborne particulate matter (PM2.5) concentration. Int. J. Environ. Res. Publ. Health 20.
- Jung, W., Lee, J., Han, S., Ko, S., Kim, T., Kim, Y., 2018. An efficient reduced grapheneoxide filter for PM2.5 removal. J. Mater. Chem. 6, 16975–16982.
- Kool, D., Kool, D., Agam, N., Lazarovitch, N., Heitman, J., Sauer, T., Ben-Gal, A., 2014. A review of approaches for evapotranspiration partitioning. Agric. For. Meteorol. 184, 56–70.
- Li, K., Li, C., Hu, Y., Xiong, Z., Wang, Y., 2023a. Quantitative estimation of the PM2.5 removal capacity and influencing factors of urban green infrastructure. Sci. Total Environ. 867, 161476.
- Li, S., He, C., Zhang, Y., Wang, L., Zhang, Y., Wei, C., Zhang, L., 2023b. Effects of different external factors on urban roadside plants for the reduction of airborne fine particulate matters. Int. J. Phytoremediation 25 (14), 1901–1912.
- Liu, L., Guan, D., Peart, M., Wang, G., Zhang, H., Li, Z., 2013. The dust retention capacities of urban vegetation—a case study of Guangzhou, South China. Environ. Sci. Pollut. Control Ser. 20, 6601–6610.
- Liu, J., Zhai, J., Zhu, L., Yang, Y., Liu, J., Zhang, Z., 2016. Particle removal by vegetation: comparison in a forest and a wetland. Environ. Sci. Pollut. Control Ser. 24.
- Liu, Y., Yu, Y., Liu, M., Lu, M., Ge, R., Li, S., Liu, X., Dong, W., Qadeer, A., 2018. Characterization and source identification of PM2.5-bound polycyclic aromatic hydrocarbons (PAHs) in different seasons from Shanghai, China. Sci. Total Environ. 644, 725–735.
- Liu, Y., Pace, R., Grote, R., 2020. Deposition and Resuspension Mechanisms into and from Tree Canopies: A Study Modeling Particle Removal of Conifers and Broadleaves in Different Cities, vol. 3.
- Liu, Y., Zhao, W., Zhang, L., Li, X., Peng, L., Wang, Z., Song, Y., Jiao, L., Wang, H., 2024.
 An assessment framework for mapping the air purification service of vegetation at the regional scale. Forests 15 (391).
- Nowak, D.J., Crane, D.E., Stevens, J.C., 2006. Air pollution removal by urban trees and shrubs in the United States. Urban For. Urban Green. 4 (3–4), 115–123.
- Nowak, D.J., Hirabayashi, S., Bodine, A., Hoehn, R., 2013. Modeled PM2.5 removal by trees in ten U.S. cities and associated health effects. Environ. Pollut. 178, 395–402.
- Nowak, D.J., Hirabayashi, S., Doyle, M., McGovern, M., Pasher, J., 2018. Air pollution removal by urban forests in Canada and its effect on air quality and human health. Urban For. Urban Green. 29, 40–48.
- Pace, R., Grote, R., 2020. Deposition and Resuspension Mechanisms into and from Tree Canopies: A Study Modeling Particle Removal of Conifers and Broadleaves in Different Cities.
- Putrada, A., Alamsyah, N., Fauzan, M., Oktaviani, I., Perdana, D., 2023. GRU for overcoming seasonality and trend in PM2.5 air pollution forecasting. 2023 Eighth International Conference on Informatics and Computing (ICIC), pp. 1–6.
- Qiao, L., Cai, J., Wang, H., Wang, W., Zhou, M., Lou, S., Chen, R., Dai, H., Chen, C., Kan, H., 2014. PM2.5 constituents and hospital emergency-room visit in Shanghai, China. Environ. Sci. Technol. 48 (17), 10406–10414.
- Ristorini, M., Guidolotti, G., Sgrigna, G., Jafari, M., Knappe, D., Garfi, V., Baldacchini, C., Timpe, A., Calfapietra, C., 2023. Nature-based solutions in post-industrial sites: integrated evaluation of atmospheric pollution abatement and carbon uptake in a German city. Urban Clim. 50, 101579.
- Rosenberg, N., Mckenney, M., Martin, P., 1989. Evapotranspiration in a greenhouse-warmed world: a review and a simulation. Agric. For. Meteorol. 47, 303–320.
- Ryu, J., Kim, J., Byeon, H., Go, T., Lee, S., 2019. Removal of fine particulate matter (PM2.5) via atmospheric humidity caused by evapotranspiration. Environ. Pollut. 245, 253–259.
- Seposo, X., Kondo, M., Ueda, K., Honda, Y., Michikawa, T., Yamazaki, S., Nitta, H., 2018. Health impact assessment of PM2.5-related mitigation scenarios using local risk coefficient estimates in 9 Japanese cities. Environ. Int. 120, 525–534.
- Shen, J.W., Cui, P.Y., Huang, Y.D., Luo, Y., Guan, J., 2022. New insights into quantifying deposition and aerodynamic characteristics of PM2.5 removal by different tree leaves. Air Qual. Atmos. Health.
- Stewart, I., Oke, T., 2012. Local climate zones for urban temperature studies. Bull. Am. Meteorol. Soc. 93, 1879–1900.
- Su, T., Lin, C., Lin, J., Liu, C., 2020. Dry deposition of particulate matter and its associated soluble ions on five broadleaved species in Taichung, central Taiwan. Sci. Total Environ. 753, 141788.
- Su, T.-H., Lin, C.-S., Lu, S.-Y., Lin, J.-C., Wang, H.-H., Liu, C.-P., 2022. Effect of air quality improvement by urban parks on mitigating PM2.5 and its associated heavy metals: a mobile-monitoring field study. J. Environ. Manag. 323, 116283.

- Sun, D., Shi, X., Zhang, Y., Zhang, L., 2020. Spatiotemporal distribution of traffic emission based on wind tunnel experiment and computational fluid dynamics (CFD) simulation. J. Clean. Prod., 124495
- Trang, T.T., Khoa, N.D., Truyền, D.M., Quyền, V.T., 2022. Evaluation of the role of trees in removing air pollutants at selected universities IN HO CHI MINH city using I-tree eco model. TNU Journal of Science and Technology 227 (15), 117–129.
- Wang, H., Shi, H., Li, Y., Yu, Y., Zhang, J., 2013. Seasonal variations in leaf capturing of particulate matter, surface wettability and micromorphology in urban tree species. Front. Environ. Sci. Eng. 7, 579–588.
- Wang, J., Zhang, L., Niu, X., Liu, Z., 2020. Effects of PM2.5 on health and economic loss: evidence from Beijing-Tianjin-Hebei region of China. J. Clean. Prod.
- Wróblewska, K., Jeong, B.R., 2021. Effectiveness of plants and green infrastructure utilization in ambient particulate matter removal. Environ. Sci. Eur. 33, 110.
- Wu, J., Wang, Y., Qiu, S., Peng, J., 2019. Using the modified i-Tree Eco model to quantify air pollution removal by urban vegetation. Sci. Total Environ. 688, 673–683.
- Xiao, Q., Ma, Z., Li, S., Liu, Y., 2015. The impact of winter heating on air pollution in China. PLoS One 10 (1), e0117311.
- Xiao, Q., Geng, G., Liu, S., Liu, J., Meng, X., Zhang, Q., 2022. Spatiotemporal continuous estimates of daily 1 km PM2.5 from 2000 to present under the Tracking Air Pollution in China (TAP) framework. Atmos. Chem. Phys. 22, 13229–13242.
- Xu, Z., Jiang, Y., Jia, B., Zhou, G., 2016. Elevated-CO2 response of stomata and its dependence on environmental factors. Front. Plant Sci. 7.
- Yan, G., Yu, Z., Wu, Y., Liu, J., Wang, Y., Zhai, J., Cong, L., Zhang, Z., 2020. Understanding PM2.5 concentration and removal efficiency variation in urban forest park—observation at human breathing height. PeerJ 8.
- Yan, K., Pu, J., Park, T., Xu, B., Zeng, Y., Yan, G., Weiss, M., Knyazikhin, Y., Myneni, R., 2021. Performance stability of the MODIS and VIIRS LAI algorithms inferred from analysis of long time series of products. Rem. Sens. Environ.
- Yang, J., Chang, Y., Yan, P., 2015. Ranking the suitability of common urban tree species for controlling PM2.5 pollution. Atmos. Pollut. Res. 6, 267–277.
- Yang, L., Li, C., Tang, X., 2020. The impact of PM2.5 on the host defense of respiratory system. Front. Cell Dev. Biol. 8.

- Yang, Z., Yang, J., Li, M., Chen, J., Ou, C., 2021. Nonlinear and lagged meteorological effects on daily levels of ambient PM2.5 and O3: evidence from 284 Chinese cities. J. Clean. Prod. 278, 123931.
- Yin, H., Pizzol, M., Jacobsen, J., Xu, L., 2018. Contingent valuation of health and mood impacts of PM2.5 in Beijing, China. Sci. Total Environ. 630, 1269–1282.
- Yin, S., Zhang, X., Yu, A., Sun, N., Lyu, J., Zhu, P., 2019. Determining PM2.5 dry deposition velocity on plant leaves: an indirect experimental method. Urban For. Urban Green.
- Zhai, H., Yao, J., Wang, G., Tang, X., 2022. Study of the effect of vegetation on reducing atmospheric pollution particles. Remote Sens. 14, 1255.
- Zhang, N., Xiong, H., Ge, X., Duan, P., Mao, X., Wang, Y., 2016. [Response of human respiratory height PM2.5 variation characteristics to meteorological factors during winter haze days in beijing]. Huan jing ke xue= Huanjing kexue 37 (7), 2419–2427.
- Zhang, X., Du, J., Huang, T., Zhang, L., Gao, H., Zhao, Y., Ma, J., 2017. Atmospheric removal of PM2.5 by man-made Three Northern Regions Shelter Forest in Northern China estimated using satellite retrieved PM2.5 concentration. Sci. Total Environ. 593–594, 713–721.
- Zhang, X., Lyu, J., Han, Y., Sun, N., Sun, W., Li, J., Liu, C., Yin, S., 2020. Effects of the leaf functional traits of coniferous and broadleaved trees in subtropical monsoon regions on PM2.5 dry deposition velocities. Environ. Pollut. 265 (Pt B), 114845.
- Zhang, B., Xie, Z., She, X., Gao, J., 2021. Quantifying the potential contribution of urban forest to PM2.5 removal in the city of Shanghai, China. Atmosphere 12 (9), 1171.
- Zhang, L., He, J., Gong, S., Guo, X., Zhao, T., Zhou, C., 2022. Effect of vegetation seasonal cycle alterations to aerosol dry deposition on PM2.5 concentrations in China. Sci. Total Environ.
- Zheng, H., Kong, S., Yan, Q., Wu, F., Cheng, Y., Zheng, S., Wu, J., Yang, G., Zheng, M., Tang, L., Yin, Y., Chen, K., Zhao, T., Liu, D., Li, S., Qi, S., Zhao, D., Zhang, T., Ruan, J., Huang, M., 2019. The impacts of pollution control measures on PM2.5 reduction: insights of chemical composition, source variation and health risk. Atmos. Environ.
- Zhou, Y., Liu, H., Zhou, J., Xia, M., 2019. GIS-based urban afforestation spatial patterns and a strategy for PM2.5 removal. Forests.